Soft Matter

Cite this: *Soft Matter*, 2011, **7**, 11416

www.rsc.org/softmatter

PAPER

On spray drying of uniform silica-based microencapsulates for controlled release

Winston Duo Wu,[a] Wenjie Liu,[a] Cordelia Selomulya[a] and Xiao Dong Chen*[ab]

Received 12th May 2011, Accepted 19th July 2011
DOI: 10.1039/c1sm05879g

Although spray drying is a scalable route for particle formation with easy product recovery, a typical spray drier produces broad distributions of particles with various morphologies in a single batch, due to the non-uniform formation of droplets, wide spray trajectories, and various residence times experienced by the droplets during drying. Thus any attempt to interpret the resulting particle functionality directly in relation to their physico-chemical properties is difficult. Here, uniform silica-based microencapsulates encapsulating vitamin B_{12} homogenously distributed within their matrix were synthesised in a single step *via* a micro-fluidic-jet-spray-dryer (MFJSD), utilising a micro-fluidic-aerosol-nozzle (MFAN) for continuous generation of monodisperse droplets. We investigated the effects of lactose and Na-alginate to the properties of the silica matrix, as well as the overall particle shapes. The uniform nature of the particles allowed direct correlations between the matrix properties and the release behaviour of vitamin B_{12} to be observed without the complications of wide size distribution or variety of shapes. Spherical particles with relatively smooth surface were obtained with lactose addition, while incorporation of Na-alginate resulted in increasing surface roughness. Lactose accelerated the release of the encapsulated vitamin B_{12} (VB12), due to the relatively fast lactose dissolution that allowed buffer to penetrate deep into the matrix to facilitate diffusion and silica erosion. On the contrary, Na-alginate slowed down the release considerably by serving as an additional barrier to decelerate the matrix erosion, as well as due to ionic attraction to the VB12 molecules. Release kinetics data indicated diffusion as the main release mechanism independent of the microencapsulate composition. The release profiles from different compositions of the synthesized particles demonstrated good agreements with the computational predictions, highlighting the ability to modulate the release behaviour directly from the precursor compositions.

Introduction

Silica as a carrier matrix has several advantages over natural[1,2] and synthetic polymers,[3] as it is relatively cheap and easy to purify, with excellent physical and chemical stabilities, good biocompatibility, and biodegradability with favourable tissue responses *in vitro* and *in vivo*.[4–6] Silica-based microencapsulates incorporating active drug components have been previously synthesized using emulsification[7] or spray drying.[8] Compared to emulsification, spray drying is scalable and offers a more efficient means to obtain practical yields in a single step. Kortesuo *et al.*[8] previously synthesised silica microencapsulates *via* spray drying to study the effects of pH of the precursor on the release rate of dexmedetomidine, as the particles formed distinct structures induced by different pH during the polymerization process of the precursor solutions. The release behaviour was proposed to depend on the different erosion rates of the silica matrix. Nevertheless, the non-uniformity of the particles restricted this interpretation since the erosion rate could also be influenced by the wide distribution of geometric sizes and the presence of agglomerated particles.[9]

We previously introduced a specially designed dryer[10,11] to fabricate microencapsulates with uniform characteristics, including size and morphology. For controlled release applications, such uniformity is beneficial since a wide size distribution could lead to undesirable burst effects.[12,13] In addition, any interpretation of particle functionalities, including release behaviour, in relation to their characteristics (and also the synthesis conditions) is difficult to conclude without the consistency in their properties and reproducibility in the processing.[14,15] Here, monodisperse silica microencapsulates in the size range of <40 μm were synthesised from aqueous precursor solutions containing hydrolyzed tetraethyl orthosilicate (TEOS) in acidic condition. Water-soluble vitamin B_{12} (VB_{12}) was selected as the encapsulated ingredient.

Two naturally existing products, lactose (small molecule disaccharide) and alginate (biomacromolecular polysaccharide)

[a]*Department of Chemical Engineering, Monash University, VIC, 3800, Australia*
[b]*Department of Chemical and Biochemical Engineering, Xiamen University, 361005, Fujian Province, P.R. China*

were used in combination of the sol–gel derived inorganic silica matrix. The incorporation of natural products should improve the biocompatibility of the products,[16] and the possibility to tailor the properties and functionalities of microencapsulates.[17] For controlled release applications, the incorporation of organic ingredients could provide additional, stimuli-responsive barriers to regulate the speed of drug liberation, and to further guarantee the desired dose of maintenance.[18,19] Silica-based materials are very stable over a range of environmental conditions, presenting some limitations when in-demand release is required. On the contrary, stimuli-responsive properties commonly exist for organic components such as polymers.[20] For hybrid silica-based materials, the insoluble silica could serve as the basic matrix, with soluble organic components as the modifier.[21]

In this work, the effects of lactose and Na-alginate, their content, and VB_{12} loading on particle size, silica matrix properties, morphology, and VB_{12} release profiles can be clearly demonstrated from systematic studies utilising uniform particles without any agglomeration.

Experimental section

Preparation of precursor solution

Tetraethyl orthosilicate (TEOS), vitamin B_{12} (VB_{12}), alpha-D-lactose monohydrate (~360 g mol^{-1}) and Na-Alginate (low viscosity, ~10 000 g mol^{-1}) were purchased from Sigma (AUS) and used without further purification. Silica sols were prepared by hydrolysing TEOS in distilled water with TEOS/water molar ratio of 14 : 1, while 0.1 M HCl was added to adjust the pH to 2.3. The hydrolysis process was conducted for 30 mins with continuous magnetic stirring, after which the sol was further diluted with distilled water to the desired content (%w/v). VB_{12}, while either α-D-lactose monohydrate or Na-Alginate was added into the transparent silica sols according to the compositions as listed in Table 1. Silica precursor without any additive (referred to as SV) was prepared as control. Precursor solutions containing lactose were referred to as SVL samples, while those containing Na alginate were referred to as SVA samples.

Generation of monodisperse droplets

Monodisperse droplets were formed by a specially designed micro-fluidic aerosol nozzle (MFAN), with orifice diameter of 25 μm. The detailed operating mechanisms have been introduced previously,[22] with the nozzle design capable of handling colloidal or liquid precursors in a continuous process. The precursor solution was kept in the reservoir connected to the nozzle *via* PVC tubes. A liquid jet was pressured out of the orifice, while the vibration generated by the piezoceramic material surrounding the nozzle broke-up the jet into small droplets. By controlling the liquid flow rate and vibrating frequency, monodisperse droplet formation could be achieved. The droplet formation process (*i.e.* jet diameter, droplet spacing, size and size distribution) was monitored by photographs taken using a digital SLR camera (Nikon, D90) with a speed-light (Nikon SB-400) and a micro-lens (AF Micro-Nikkon 60mm f/2.8D). Image processing and analysis software in Java (ImageJ™) was used to analyse the photographs.

Table 1 Compositions of the precursor solution for spray drying

Sol	Silica (TEOS) %w/v	VB_{12} %w/v	Lactose %w/v	Na-Alginate %w/v	Total mass content %w/v	VB_{12} content wt (%)
SV	1	0.1	0	0	1.1	9.09
SVL1	1	0.1	0.5	0	1.6	6.25
SVL2	1	0.1	1.0	0	2.1	4.76
SVL3	1	0.2	1.0	0	2.2	9.09
SVL4	1	0.3	1.0	0	2.3	13.24
SVA1	1	0.1	0	0.5	1.6	6.25
SVA2	1	0.1	0	1.0	2.1	4.76
SVA3	1	0.2	0	1.0	2.2	9.09
SVA4	1	0.3	0	1.0	2.3	13.24

Fabrication of microencapsulates

The schematic of micro-fluidic-jet-spray-dryer (MFJSD) is shown in Fig.1. The dryer chamber was made of plexiglass, while drying air heated by two parallel air heaters was blown through four main hot air inlets. A hot air dispenser was firmly fixed on top of the MFJSD (Fig.1 (inset)), with 5 mm diameter holes drilled underneath the air dispenser to uniformly distribute the hot air into the chamber. The hot air flow rate was designed in the range between 0.1 to 0.8 m s^{-1}. Six thermocouples were attached to the chamber to monitor the drying temperature distribution, while a humidity sensor was used to measure the relative humidity at the dryer outlet. For particle collection, a plate of standard steel weirs (Fig.1 (inset)) connected to an electrode was mounted at the end of the cone to charge the passing particles. A powder collection plate was connected to another electrode to attract the charged particles. The dryer inlet and outlet temperatures were maintained at 80 °C and 40 °C, respectively.

Particle characterization

Field scanning electron microscopy (FESEM, JEOL JSM-7001F, Japan) operated at 10kV was used to obtain information on particle size and morphology. As-prepared particles were coated with ~3 nm thick gold layer in argon environment at low pressure (~0.02 mbar). Particle size distribution was acquired by analysing FESEM images containing over 1000 particles using ImageJ™. The average particle size ($\bar{d}$) was defined as $\bar{d} = \sum_{i=1}^{n} \frac{d_i}{N}$ and the span of size distribution was described as $\text{Span} = \frac{d_{90} - d_{10}}{d_{50}}$, where d_i was the diameter of the i-th particle, N was the total number were the cumulative particle sizes at 90%, 50%, and 10%, respectively. FESEM energy dispersive X-ray photoelectron spectrometer (EDX) was conducted for 180 s for each sample to verify the presence of chemical element types and distributions, where atoms Si and N determining the locations of silica and VB_{12}, respectively.

VB_{12} release and silica matrix erosion profiles

The VB_{12} release and silica matrix erosion profiles of the microencapsulates (each data point represented an average obtained from studies conducted in triplicate) were monitored by mixing 100 mg of the microencapsulates with 200 ml of 0.01M phosphate buffered saline (PBS) consisting of 0.138M NaCl and 0.0027M KCl (Sigma (AUS), Inc.) as the dissolution medium at the physiological pH of

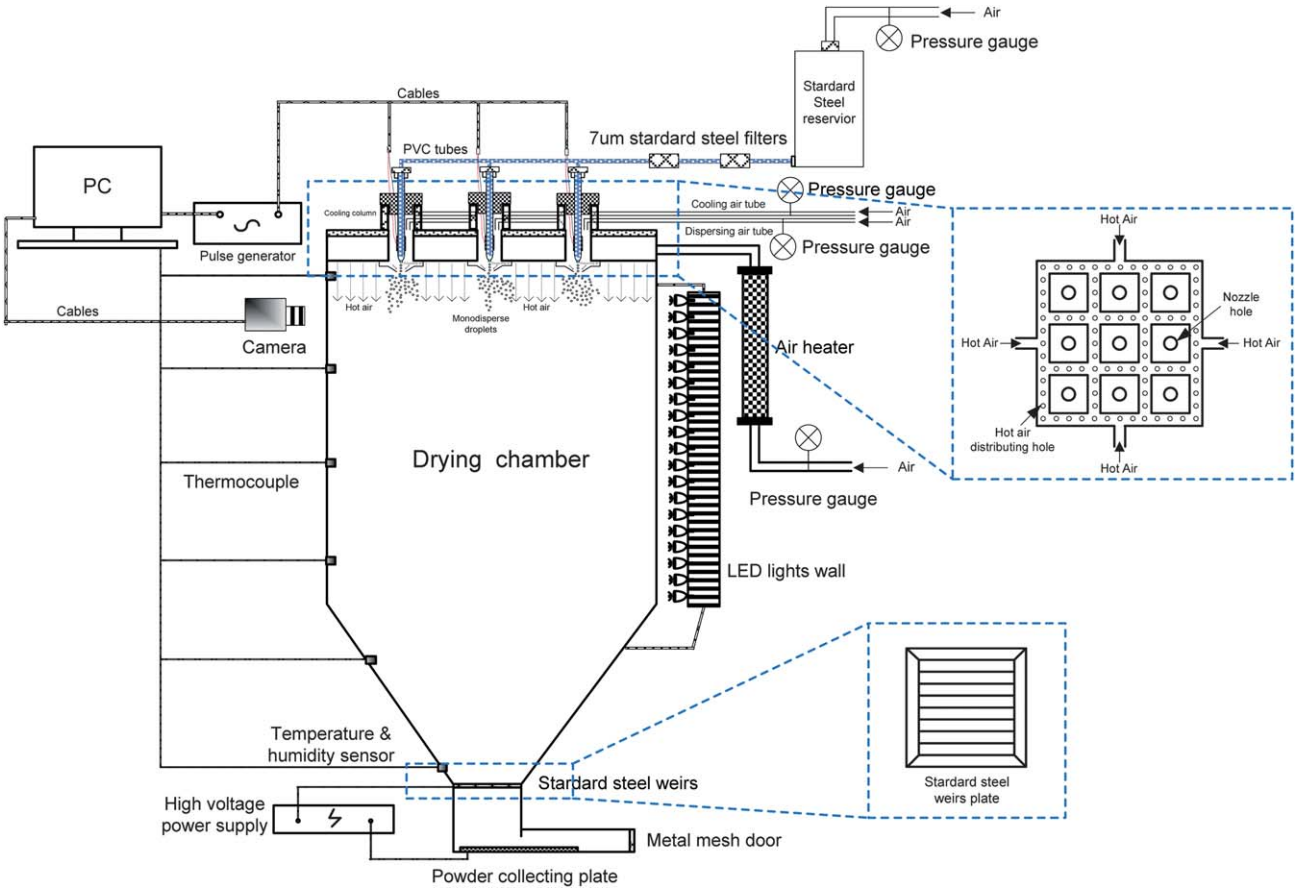

Fig. 1 Schematic graph of the microfluidic jet spray dryer.

7.4. The rotational speed was set at 20 rpm while the temperature of the water bath was maintained at 37 °C. The dissolved VB_{12} and Si $(OH)_4$ were determined by measuring the absorbance values using an fluorescence spectroscopy (SpectraMax M2/M2^e, MDS Inc., Australia) at 361 nm[23] and 820 nm,[24] respectively.

Release kinetics modeling

Experimental data from VB_{12} release profiles were fitted using different kinetics models to determine the dominant release mechanism(s). The mathematical models used as followed were zero-order kinetic (eqn (1)), first-order model (eqn (2)), square root of time equation (Higuchi equation, eqn (3)), Korsmeyer equation (eqn (4)), and Peppas-Sahlin equation (eqn (5)).[12,25–28] The first three models are represented by:

$$Q = k_0 t \tag{1}$$

$$\ln(100 - Q) = \ln Q_0 - k_1 t \tag{2}$$

$$Q = k_H t^{1/2} \tag{3}$$

where Q is the percent of encapsulated component released at time t and k_0, k_1, and k_H are the coefficients (intercept) of the equations. The Korsmeyer equation can be written as:

$$\frac{M_t}{M_\infty} = kt^n \tag{4}$$

where M_t/M_∞ is the fraction of component release at time t; k is the release rate constant; and n is the release exponent indicative of the mechanism of release. For spherical particles, a Fickian/diffusion controlled release is implied when $n = 0.43$. Accordingly, $0.43 < n < 0.85$ is an indication of both diffusion controlled release and swelling controlled release (also known as anomalous transport), while a value of n equal to 0.85 indicates case-II transport relating to polymer relaxation (gel swelling). The Peppas-Sahlin model takes the form of:

$$\frac{M_t}{M_\infty} = k_1 t^m + k_2 t^{2m} \tag{5}$$

$$\frac{R}{F} = \frac{k_2 t^m}{k_1} \tag{6}$$

where k_1, k_2 and m are constants; F represents the case-II relaxational contribution while R represents the Fickian diffusional contribution. If R/F is significantly high, then the release mechanism is relaxation-dependent; while diffusion prevails if R/F is significantly low.[29]

Results and discussion

Monodisperse droplet formation

High-speed photographs (Fig. 2) were taken to monitor the monodisperse droplet formation, with some of the data

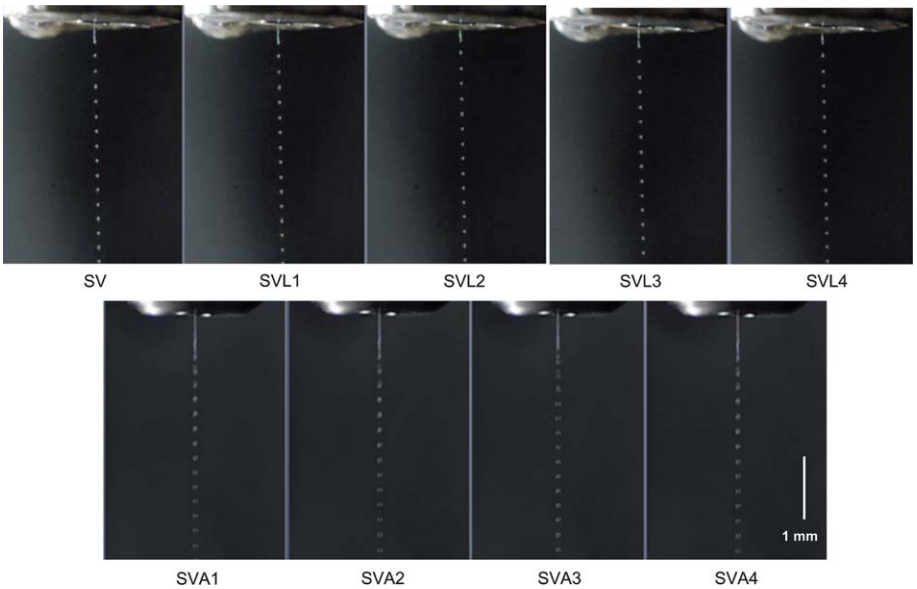

Fig. 2 High speed photographs of monodisperse droplets from different precursor solution generated using the microfluidic aerosol nozzle.

presented in Table 2. Different loadings of VB_{12} did not affect the droplet size, nor the morphology or size of the dried particles, hence only those with lactose and Na-alginate (SVL1-2, SVA1-2) were listed here. Although they were generated at equal mass flow rates, the droplet size for precursor containing Na-alginate was larger than those containing lactose, since Na-alginate induced higher viscosity of the SVA solution (40.35 cP) compared to the viscosity of the SVL solution (2.61 cP).[22]

Table 2 Droplet/particle size and particle morphology

Sol	Droplet size (μm)	Particle size (μm)	Particle morphology
SV	53.1 ± 1.2	11.0 ± 1.6	Bowl-like & smooth
SVL1	54.3 ± 1.1	14.6 ± 1.2	Dimpled & smooth
SVL2	51.6 ± 1.0	24.1 ± 1.0	Apple-like & smooth
SVA1	72.5 ± 1.4	27.1 ± 1.3	Buckled & smooth
SVA2	89.1 ± 1.7	37.5 ± 1.7	Buckled & wrinkled

Effects of lactose and alginate on particle size and morphology

Table 2 summarises the size and morphology for SV, SVL1, SVL2, SVA1 and SVA2 samples. Spray-dried neat silica microencapsulates (SV) displayed bowl-like morphology, each with a singular large hole on the surface. The particles were relatively fragile, with significantly fragmented portions (Fig. 3a). Particles doped with 0.5%w/v lactose (SVL1) had dimpled morphology without apparent fragmentation (Fig. 3b), whereas SVL2 particles with double the lactose content had smooth, almost spherical morphology with a small hole on the surface (Fig. 3c). The mean sizes of SVL1 and SVL2 particles were 14.6 ± 1.2 μm and 24.1 ±

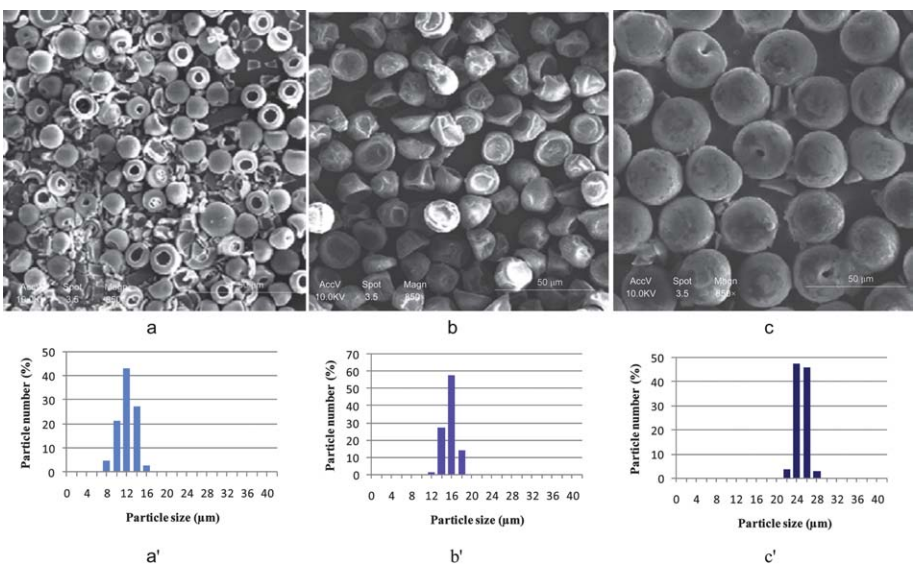

Fig. 3 FESEM images and size distribution of particles spray dried from SV (a, a′), SVL1 (b, b′) and SVL2 (c, c′) precursor solutions.

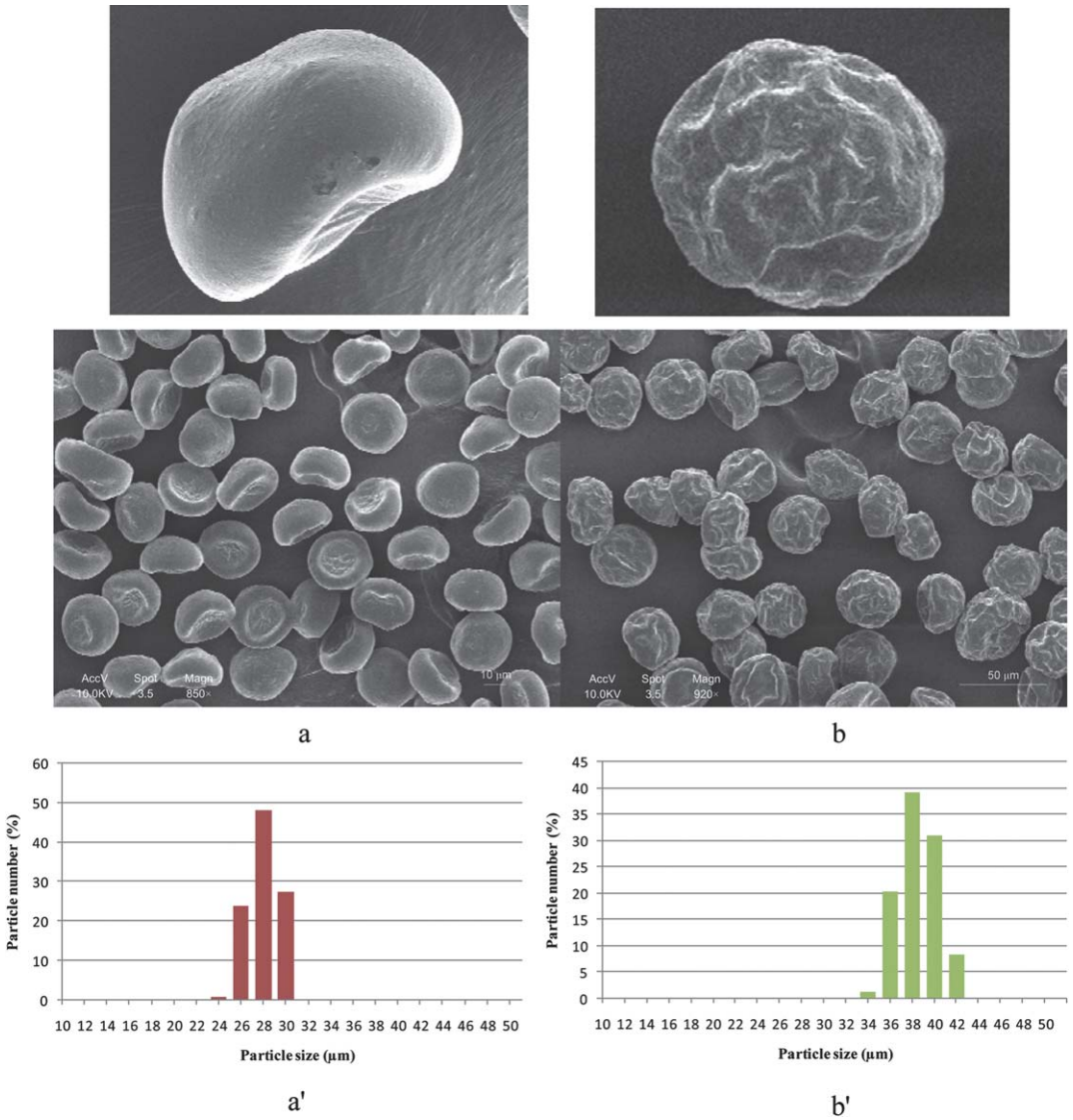

Fig. 4 FESEM images and size distribution of particles spray dried from SVA1 (a, a′) and SVA2 (b, b′) precursor solutions.

1.0 μm, respectively, with narrow size distributions (Fig. 3 (a′, b′, c′)). As monodisperse droplet generation with similar sizes and drying conditions were used to manufacture these particles, the

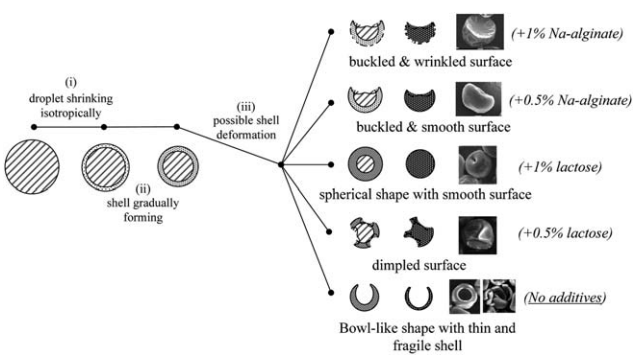

Fig. 5 Schematic illustrating the formation of different morphologies of uniform particles produced in different batches.

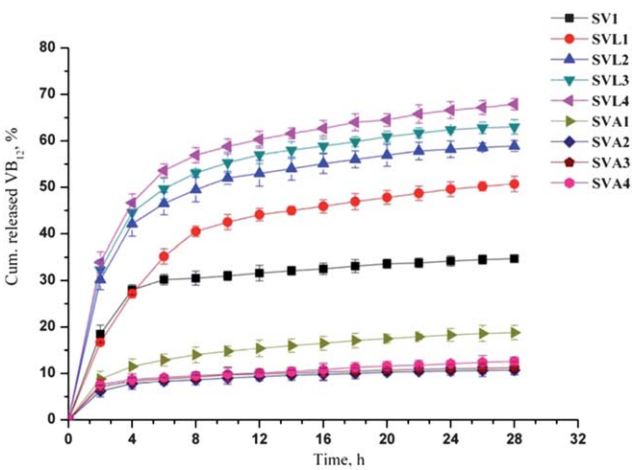

Fig. 6 Cumulative *in vitro* release of VB_{12} from spray-dried microparticles. The data represent average values from triplicate experiments.

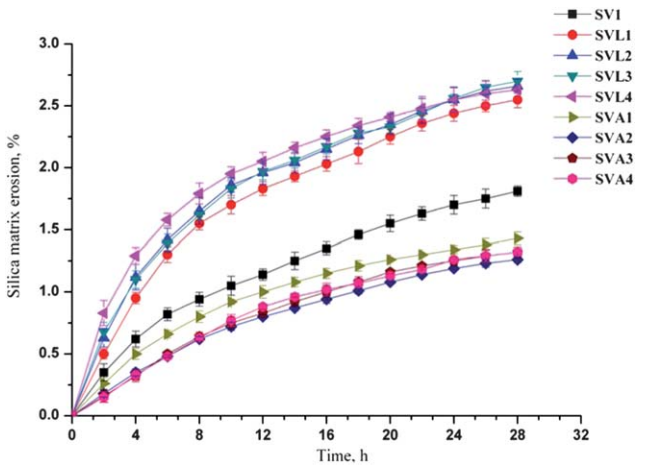

Fig. 7 Erosion profiles of silica matrix. The data represent average values from triplicate experiments.

more regular morphology and larger particle size could be directly linked to the increasing amount of lactose. In addition, distinct morphology was observed for spray-dried microencapsulates containing Na-alginate. SVA1 particles were smooth and almost platelet-like (Fig. 4a), while SVA2 particles were relatively wrinkled (Fig. 4b).

The mechanism(s) of particle formation with different morphologies *via* spray drying has been previously detailed.[10,11,30] The droplet usually experiences three drying stages, namely (1) solvent is evaporated while the droplet shrinks isotropically; (2) droplet surface is gradually populated by the solutes, forming a shell; (3) further evaporation removes moisture from inside the droplet and exerts compressive capillary stresses on the shell, which could induce surface deformation. Such deformation may also be caused from the enlargement of surface area to match the high evaporation rate. With such dependence on the mechanical property of the shell, the particles could form different morphologies. As illustrated in Fig. 5, silica particles (SV) formed bowl-like shape with a thin shell, some of which were broken due to the low solid content (1.1 wt%) that failed to provide enough mechanical integrity during surface deformation.[31] By adding lactose into the precursor, the initially formed shell was strengthened to resist compressive stresses, rendering the morphology more regular, in good agreement with the spherical pure lactose particles produced in similar conditions.[10] The existence of Na-alginate helped form visco-elastic shell subjected to buckling due to a continuously receding surface. With higher Na-alginate content, the particle surface (SVA2) appeared wrinkled as higher solid content led to early shell formation that resisted isotropical shrinkage with further drying. Here we can clearly deduce the impacts of lactose and Na-alginate, on the spray-dried particle formation and the final particle morphologies, due to the uniformity of particles generated in each batch, in contrast to previous studies with wide particle distribution and aggregation.[32–34]

Effects of lactose and alginate on VB_{12} release from microencapsulates

The release behaviour of VB_{12} from microencapsulates directly demonstrated the effects of lactose and Na-alginate (Fig. 6). Addition of lactose accelerated the release, while the equivalent amount of Na-alginate decelerated the release. Such effects became more apparent with higher adding contents. With identical VB_{12} loadings (9.09%), SV particles showed its release of 30.3% in the first 8 h, whereas SVL3 and SVA3 particles released 53.1% and 9.2%, respectively. The release profiles were also supported by the silica matrix erosion data (Fig. 7). Lactose addition elevated the erosion rate regardless of the amount, whereas Na-alginate rendered slower matrix erosion. On the other hand, different VB_{12} loadings seemed to have less impact on the drug release profile or the matrix erosion rate for particles containing either lactose or Na-alginate.

The release from the silica matrix was governed by diffusion and simultaneous matrix erosion.[35] Initial VB_{12} release from each sample could be ascribed to the existence of VB_{12} molecules close to the particle surface. EDX results (Fig. 8) indicated homogeneous distribution of VB_{12} (determined by the atom N) within the matrix with little variation with drug loading, which could explain the negligible impact of different VB_{12} loadings on the release or matrix erosion profiles. As shown in Fig. 9, the presence of lactose in SVL particles facilitated VB_{12} release, most likely due to the fast dissolution of lactose molecules on the particle surface, which allowed buffer penetration and consequently the exposure of more VB_{12} molecules within the inner matrix. On the other hand, the retarding effects of Na-alginate on VB_{12} release (SVA) was the result of a continuous hydrated alginate layer formed on the particle surface, in good agreement with Hodsdon *et al.*'s work.[36] Within 28 h of the release test, there were cumulatively 10.7%, 11.2%, 12.6%, and 12.8% of VB_{12} released from the SVA1-SVA4 particles, respectively. In a buffer

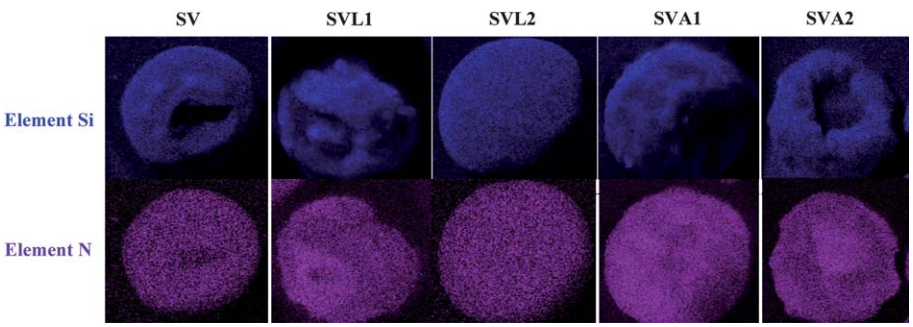

Fig. 8 EDX data demonstrating the distribution of Si and N atoms within SV, SVL1, SVL2, SVA1, and SVA2 particles.

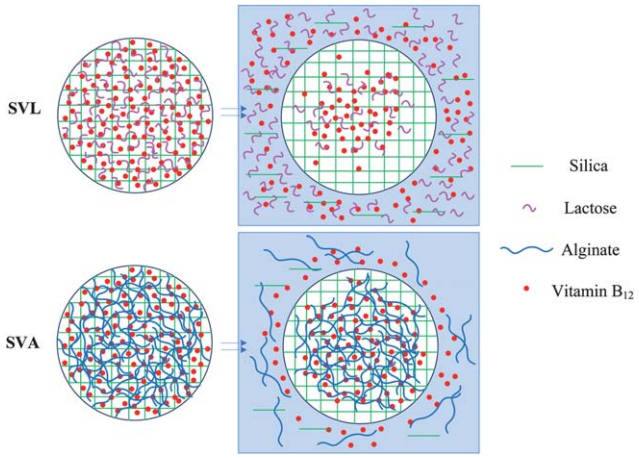

Fig. 9 Proposed mechanisms of VB_{12} release and silica matrix erosion for SVL and SVA particles. While dissolution of lactose (SVL) accelerated the release by allowing buffer to penetrate and erode the matrix, alginate layer (SVA) served as additional barrier to hydration within the internal matrix, only releasing VB_{12} close to the surface.

at pH of 7.4, Na-alginate molecules could undergo hydration and coalescence to form a continuous, viscous surface gel layer, similar to other hydrophilic polymer systems.[37,38] This alginate layer may provide another barrier to the liquid, thus prolonging the release of encapsulated ingredient in the matrix. Another plausible reason for the retarding effects observed for Na-alginate could be caused by the electrostatic interaction between VB_{12} molecules with the alginate polymer chains. The cobalt atoms in VB_{12} carries partially positive charge,[39,40] while alginate is a well known anionic polyelectrolyte due to the existence of –COOH groups on molecular chains. These specific molecular electric properties would induce somewhat affinity among these molecules, thus restricting the release.[41]

Modelling the release kinetics

The release data could be directly compared with those predicted by empirical kinetic models for uniform-sized particles to verify the dominant release mechanism(s). The kinetic parameters (Table 3) were obtained using eqn (2)–(6). Although it has been suggested that release of water-soluble molecules from silica matrix was diffusion-dominated,[35,42] we found that there was no effective correlation with any kinetic model for SV particles. The first-order model was well fitted for both SVL and SVA particles with the correlation coefficients from 0.9756 to 0.9840 and 0.9901 to 0.9985, respectively. It implied that despite the relatively fast initial VB_{12} release due to lactose dissolution, SVL particles could maintain the diffusion-controlled release manner for longer periods. On the other hand, the addition of Na-alginate did not alter the diffusion-controlled release mechanism, much likely due to the role of alginate as a barrier within the matrix.

Better fit was achieved using Korsmeyer model for SVA particles with the correlation coefficients between 0.9765 and 0.9911. However, the value range of n was from 0.1661 to 0.2736, considerably differing from the theoretical value of 0.43 that characterized diffusion-controlled release mechanism from mono-sized spherical powders with non-swellable matrix. Given that the SVA particles had narrow size distributions with non-swellable silica matrix, the variation of the n values could be due to the shapes of these particles.[13]

The predominance of diffusion governing the release mechanisms of both SVL and SVA particles was further confirmed by examining the release data with the Peppas-Sahlin model (eqn (5) and (6)), as shown in Fig. 10. For SVA3, SVA4 particles, the R/F ratios were very low (<0.059), indicating that the release kinetics was mainly controlled by diffusion. The release from the SVL3, SVL4 particles was characterized by much higher R/F (<0.554), but the value was still low enough to imply diffusion-dependant

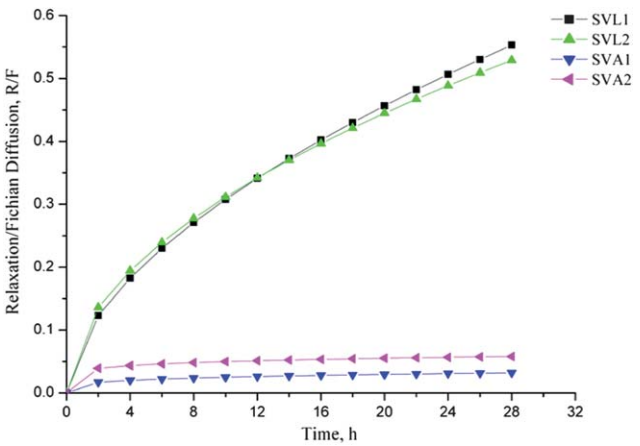

Fig. 10 R/F ratio values plotted against time for SVL1, SVL2, SVA1 and SVA2 particles.

Table 3 VB_{12} release kinetic model parameters of spray-dried samples

	First-order model		Higuchi model		Korsmeyer model			Peppas-Sahlin model		
Sample code	k_1	R^2	k_H	R^2	k	R^2	n	k_1	k_2	m
SV	0.0809	0.8610	7.2651	0.6521	0.1845	0.7537	0.2836	0.1277	−0.0129	0.5310
SVL1	0.1826	0.9792	10.4740	0.8575	0.1925	0.8667	0.3962	0.1334	−0.0094	0.6132
SVL2	0.1765	0.9770	10.8690	0.8139	0.2259	0.8751	0.3417	0.1580	−0.0129	0.5714
SVL3	0.2005	0.9760	11.8080	0.8050	0.2413	0.8546	0.3438	0.1731	−0.0143	0.5700
SVL4	0.2300	0.9840	13.2520	0.7730	0.2923	0.8729	0.3034	0.2224	−0.0212	0.5150
SVA1	0.0443	0.9980	4.0543	0.8285	0.1140	0.9896	0.2736	0.0790	−0.0074	0.3838
SVA2	0.0182	0.9940	2.4023	0.6294	0.0888	0.9805	0.1944	0.0624	−0.0083	0.2940
SVA3	0.0169	0.9967	2.5317	0.5422	0.0992	0.9911	0.1661	0.0731	−0.0010	0.2435
SVA4	0.0216	0.9901	2.7731	0.6672	0.1009	0.9840	0.1905	0.0488	−0.0017	0.1482

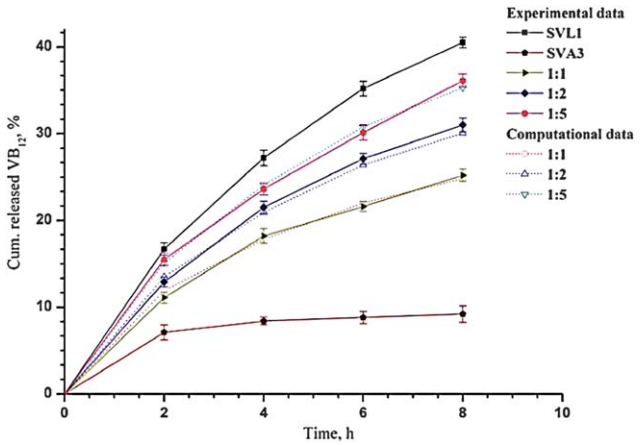

Fig. 11 VB_{12} release profiles from experimental and computational data for SVL1 and SVA3 particles, as well as their mixtures in ratio of 1 : 1, 1 : 2, 1 : 5 and 1 : 10 (w/w). Filled symbols: experimental data; open symbols: computational data.

release mechanism.[29] No significant differences in terms of main release mechanism were observed at different VB_{12} loadings.

We also demonstrated the added advantage of this methodology in producing uniform microencapsulates for controlled release. Here we mixed SVL1 and SVA3 particles in the mass proportions of 1 : 1, 1 : 2, 1 : 5 and 1 : 10. The release profiles of the mixed samples were experimentally measured and then compared with the computational data obtained by the weighted-average combinations of SVL1 and SVA3 particles. Excellent agreement with the predicted data (Fig. 11) indicated that the release profile of the encapsulated component could be easily modulated by mixing different samples of known sizes and mass proportions, due to the reproducibility of uniform particle produced here.

Conclusion

Uniform and non-agglomerated VB_{12}/silica microencapsulates (<40 μm) were successfully synthesized using a specially designed spray dryer. The uniformity of the particles allowed a clear demonstration of the effects of α-D-lactose monohydrate and Na-alginate as part of the matrices on the spray-dried particle size, morphology, and VB_{12} release behaviour. In general, the particle size increased with higher amount of additive regardless of the additive type. The addition of lactose facilitated the formation of spherical particles with relatively smooth surface, whereas Na-alginate rendered the particles buckled with either smooth or rough surface, depending on the additive content. VB_{12} release profiles indicated that lactose accelerated release, while Na-alginate had the opposite effect by serving as an additional barrier to hydration. Homogeneous distributions of VB_{12} molecules within the matrix could be achieved at various loadings and had little effects on the release profiles. The results from empirical kinetics modelling suggested a diffusion-dependant release mechanism for microencapsulates containing lactose and Na-alginate. The release behaviour from mixtures of uniform microencapsulates also corresponded directly to the linear weighted combination of the individual release profiles, due to the good reproducibility of the uniform particle produced here, illustrating the ability to control the release rate.

Acknowledgements

The authors acknowledge financial support from the Australian Research Council (ARC Discovery Grant DP0773688).

References

1 C. Oussoren and G. Storm, *Adv. Drug Delivery Rev.*, 2001, **50**, 143–156.
2 K. Kataoka, A. Harada and Y. Nagasaki, *Adv. Drug Delivery Rev.*, 2001, **47**, 113–131.
3 P. Couvreur, C. Dubernet and F. Puisieux, *Eur. J. Pharm. Biopharm.*, 1995, **41**, 2–13.
4 S. Radin, G. El-Bassyouni, E. J. Vresilovic, E. Schepers and P. Ducheyne, *Biomaterials*, 2005, **26**, 1043–1052.
5 K. P. Peterson, C. M. Peterson and E. J. A. Pope, *Proc. Soc. Exp. Biol. Med.*, 1998, **218**, 365–369.
6 P. Kortesuo, M. Ahola, M. Kangas, T. Leino, S. Laakso, L. Vuorilehto, A. Yli-Urpo, J. Kiesvaara and M. Marvola, *J. Controlled Release*, 2001, **76**, 227–238.
7 S. Radin, T. Chen and P. Ducheyne, *Biomaterials*, 2009, **30**, 850–858.
8 P. Kortesuo, M. Ahola, M. Kangas, M. Jokinen, T. Leino, L. Vuorilehto, S. Laakso, J. Kiesvaara, A. Yli-Urpo and M. Marvola, *Biomaterials*, 2002, **23**, 2795–2801.
9 E. M. Santos, S. Radin and P. Ducheyne, *Biomaterials*, 1999, **20**, 1695–1700.
10 W. D. Wu, R. Amelia, N. Hao, C. Selomulya, D. Y. Zhao, Y.-L. Chiu and X. D. Chen, *AIChE J.*, 2011, DOI: 10.1002/aic.12489.
11 W. Liu, W. D. Wu, C. Selomulya and X. D. Chen, *Soft Matter*, 2011, **7**, 3323–3330.
12 R. H. Guy, J. Hadgraft, I. W. Kellaway and M. Taylor, *Int. J. Pharm.*, 1982, **11**, 199–207.
13 P. L. Ritger and N. A. Peppas, *J. Controlled Release*, 1987, **5**, 23–36.
14 L. X. Liu, I. Marziano, A. C. Bentham, J. D. Litster, E. T. White and T. Howes, *Int. J. Pharm.*, 2008, **362**, 109–117.
15 N. Y. K. Chew and H.-K. Chan, *Pharm. Res.*, 2001, **18**, 1570–1577.
16 I. Šimkovic, *Carbohydr. Polym.*, 2008, **74**, 759–762.
17 S. B. Park, J. O. You, H. Y. Park, S. J. Hamm and W. S. Kim, *Biomaterials*, 2001, **22**, 323–330.
18 A. C. S. Alcantara, P. Aranda, M. Darder and E. Ruiz-Hitzky, *J. Mater. Chem.*, 2010, **20**, 9495–9504.
19 J. M. Xue, C. H. Tan and D. Lukito, *J. Biomed. Mater. Res., Part B*, 2006, **78B**, 417.
20 Y. L. Li, D. Maciel, H. Tomas, J. Rodrigues, H. Ma and X. Y. Shi, *Soft Matter*, 2011, **7**, 6231.
21 M. Gimeno-Fabra, M. Peroglio, D. Eglin, M. Alini and C. C. Perry, *J. Mater. Chem.*, 2011, **21**, 4086.
22 W. D. Wu, S. X. Q. Lin and X. D. Chen, *AIChE J.*, 2011, **57**, 1386–1392.
23 H. A. O. Hill, J. M. Pratt, R. G. Thorp, B. Ward and R. J. P. Williams, *Biochemical J.*, 1970, **120**, 263–269.
24 O. G. Koch and G. A. Koch-Dedic, *Handbuch der Spurenanalyse*, Springer, Berlin, 1974.
25 T. Higuchi, *J. Pharm. Sci.*, 1963, **52**, 1145–1149.
26 N. A. Peppas and J. J. Sahlin, *Int. J. Pharm.*, 1989, **57**, 169–172.
27 J. Siepmann and N. A. Peppas, *Adv. Drug Delivery Rev.*, 2001, **48**, 139–157.
28 C. Liu, K. G. Desai, X. Tang and X. Chen, *Drying Technol.*, 2006, **24**, 769–776.
29 R. Bettini, P. Colombo, G. Massimo, P. L. Catellani and T. Vitali, *Eur. J. Pharm. Sci.*, 1994, **2**, 213–219.
30 R. Vehring, W. R. Foss and D. Lechuga-Ballesteros, *J. Aerosol Sci.*, 2007, **38**, 728–746.
31 D. Lechuga-Ballesteros, A. Bakri and D. Miller, *Pharm. Res.*, 2003, **20**, 308–318.
32 H. Takeuchi, S. Nagira, H. Yamamoto and Y. Kawashima, *Int. J. Pharm.*, 2005, **293**, 155–164.
33 N. Tsapis, D. Bennett, B. Jackson, D. A. Weitz and D. A. Edwards, *Proc. Natl. Acad. Sci. U. S. A.*, 2002, **99**, 12001–12005.

34 D. O. Corrigan, A. M. Healy and O. I. Corrigan, *Int. J. Pharm.*, 2002, **235**, 193–205.
35 P. Kortesuo, M. Ahola, M. Kangas, A. Yli-Urpo, J. Kiesvaara and M. Marvola, *Int. J. Pharm.*, 2001, **221**, 107–114.
36 A. C. Hodsdon, J. R. Mitchell, M. C. Davies and C. D. Melia, *J. Controlled Release*, 1995, **33**, 143–152.
37 I. Katzhendler, R. Azoury and M. Friedman, *J. Controlled Release*, 1998, **54**, 69–85.
38 D.-H. Kim and D. C. Martin, *Biomaterials*, 2006, **27**, 3031–3037.
39 G. N. Schrauzer, *Angew. Chem., Int. Ed. Engl.*, 1976, **15**, 417–426.
40 L. S. Beckmann and D. G. Brown, *Biochim. Biophys. Acta, Gen. Subj.*, 1976, **428**, 720–725.
41 M. Leonard, M. R. De Boisseson, P. Hubert, F. Dalençon and E. Dellacherie, *J. Controlled Release*, 2004, **98**, 395–405.
42 T. Czuryszkiewicz, S. Areva, M. Honkanen and M. Lindén, *Colloids Surf., A*, 2005, **254**, 69–74.

